

ABS-0116

Traffic noise radiation suppression in an un baffled long enclosure using micro-perforated panel

Weiping YANG¹; Yatsze CHOY²; Ying LI³

^{1, 2, 3} The Hong Kong Polytechnic University, Hong Kong, P. R. China

ABSTRACT

Sound radiation control of an un baffled long enclosure using corrugated Z-shaped micro-perforated panel absorbers (ZMPPAs) is investigated. First, a hybrid model based on the finite element method (FEM) and the Wiener-Hopf (WH) technique is established to calculate the sound pressure level (SPL) radiated from an un baffled long enclosure. Subsequently, an array of ZMPPAs is proposed to absorb higher-order acoustical modes inside the long enclosure so that the radiated noise can be suppressed. After that, the sound attenuation performance of ZMPPAs is evaluated and compared with that of corrugated and flat microperforated panel absorbers (CMPPAs, FMPPAs). The results demonstrate that ZMPPAs can reduce the radiated SPL within a wide frequency range which is favorable for the suppression of environmental noise. Finally, the performance of the ZMPPAs, CMPPAs, and FMPPAs in reducing the radiated noise from an un baffled long enclosure is examined using a quasi-2D test rig. The experimental results coincide well with the calculated results which validates the proposed model and verifies part of the numerical findings.

Keywords: Sound suppression, Un baffled long enclosure, Micro-perforated panel absorber

1. INTRODUCTION

Sound radiation control of an un baffled long enclosure has been an important research subject in recent years as this scenario could be widely seen in the reduction of environmental noise. Helmholtz resonators (HRs) have been proposed to suppress the sound peaks inside the un baffled long enclosure so that the radiated SPL field around the resonant frequencies of the HRs could be attenuated (1). The noise reduction performance of an array of HRs, however, is still unsatisfactory which is limited by their narrow working frequency bandwidths. Therefore, for the control of noise radiated from a long enclosure, a simple, compact, and broadband noise suppression device is needed. The feasibility of applying two-dimensional hard rough surfaces to attenuate the noise level inside a long enclosure has been examined by Law et al. (2). It was observed that an average sound reduction of about 3 dB over the frequency range from 500 Hz to 5000 Hz could be obtained. Aiming at absorbing the higher-order acoustical modes inside a duct, the interactions between acoustical modes and a perforated liner were investigated by Eldredge (3). Later, enlightened by the research of Eldredge, broadband acoustical liners with multiple cavity resonances were designed and the acoustical performance of the liners was investigated (4, 5). From above-mentioned findings, acoustical liners consisting of micro-perforated panel absorbers (MPPAs) are promising noise control devices to attenuate the noise that is consisting of higher-order acoustical modes. Apart from applying multiple cavity resonances, MPPAs integrated with trapezoidal (6) and L-shaped (7) cavities were also proposed. More acoustical modes that are initially decoupled with the MPP backed by a rectangular cavity are coupled with the MPP backed by cavities with irregular shapes. Compared with a flat MPPA (FMPPA) backed by constant air gap, the irregular-shaped MPPAs provide more spectral peaks and achieve good absorption performance at the dips in the sound absorption coefficient curve. These designs are from the perspective of the backing cavity and the incident plane waves are normal to the MPP. However, in practice, the distribution of sound pressure fields is complex in a duct, enclosure, and cavity system. The amplitudes and incident angles of sound pressure along MPP surfaces are different. Consequently, the in-situ performance of

¹ w.p.yang@connect.polyu.hk

² mmyschoy@polyu.edu.hk

³ carlos.li@connect.polyu.hk

the MPPAs is usually inferior to the theoretical results as the normal sound absorption coefficient of the MPPAs is inapplicable. Hence, to investigate the performance of an MPPA in practical acoustical environments, researches on the performance of MPPAs under oblique and random plane-wave incidences have been carried out (8, 9, 10). Results show that shape designs of cavities are not enough for a broadband sound absorption performance of an MPPA, especially when the sound waves are impinging tangentially or at a large incident angle on the flat MPP. To further improve the sound absorption performance of an MPPA under an oblique plane-wave incidence or in the diffuse field, a corrugated MPPA (CMPPA) with a sinusoidal MPP profile is proposed (11). Both the plane-wave incident angle to the local surface and the cavity shape of the MPPA are changed by introducing the corrugated MPP, which enhanced the sound absorption at the troughs and more spectral peaks can be observed. A key parameter that influences the sound absorption performance of a CMPPA is the corrugation depth. The corrugated profile of MPP, however, is determined when the corrugation depth of the MPP and the width of the MPPA are chosen, which lacks flexibility for higher sound absorption performance. To find a more flexible configuration of the corrugated MPP profile, a Z-shaped micro-perforated panel absorber (ZMPPA) is proposed here. It is targeted for the absorption of higher-order acoustical modes inside an unbaﬄed long enclosure so that the radiated sound field can be attenuated accordingly. In addition to the advantages of CMPPAs, a ZMPPA is more versatile, which is promising for broadband noise control in large spaces and buildings.

The remainder of this paper is organized as follows. A hybrid model is first proposed to calculate the sound radiation from unbaﬄed long enclosures integrated with MPP absorbers. Subsequently, the sound suppression performance of the ZMPPA is investigated and compared with that of FMPPA and CMPPA. Finally, experimental results are presented to validate the numerical model and examine the performance of the ZMPPA. Results show that the ZMPPA can attenuate the radiated noise within a wide frequency range which proves that the ZMPPA is a promising noise control device in practical applications.

2. HYBRID MODEL

To investigate the sound absorption performance of MPPAs inside a long enclosure, a hybrid method based on the finite element (FE) method and Winer-Hopf (WH) technique is established. The schematic diagram of an FE-WH-based hybrid method to predict the sound radiated from an unbaﬄed long enclosure integrated with MPPAs is shown in Figure 1. The sound pressure field inside a long enclosure is obtained by the FEM, while the radiated sound pressure field is determined by the W-H technique using the calculated pressure and particle velocity at the opening.

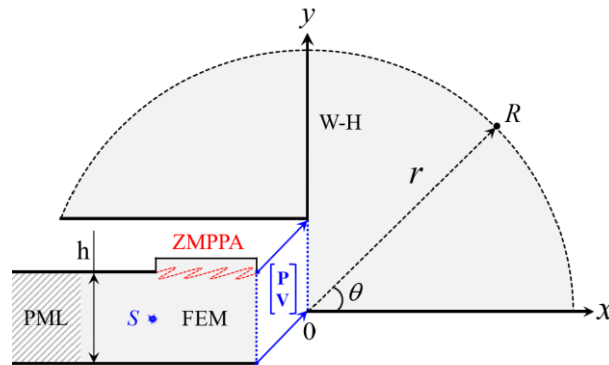


Figure 1 – Schematic diagram of a hybrid method to predict sound radiation from an unbaﬄed long enclosure with the ground.

The W-H solution for the rigid unbaﬄed long enclosure with the ground is obtained as follows:

$$\dot{P}^+(\alpha, h) = \sum_{m=0}^{\infty} (-1)^m \frac{f_m - i\alpha_m g_m}{2\alpha_m (\alpha + \alpha_m)} L^+(\alpha_m) \kappa^+(\alpha_m) L^+(\alpha) \kappa^+(\alpha) \quad (1)$$

where $L^+(\alpha)$ and $\kappa^+(\alpha)$ are kernel functions which are expressed as

$$L^+(\alpha) = \sqrt{\frac{\sin(kh)}{k}} \times \exp \left\{ \ln \left[\frac{\alpha - i\kappa(\alpha)}{k} \right] \frac{\kappa(\alpha)h}{\pi} \right\} \quad (2)$$

$$\times \exp \left\{ \left(1 - C - \ln \left(\frac{2\pi}{kh} \right) - \frac{i\pi}{2} \right) \frac{i\alpha h}{\pi} \right\} \times \prod_{l=1}^{\infty} \left(1 + \frac{\alpha}{\alpha_l} \right) \times \exp \left(-\frac{i\alpha h}{l\pi} \right) \quad (3)$$

$$\kappa^+(\alpha) = k + \alpha$$

The far-field directivity pattern of the radiated sound pressure field outside the unbaffled long enclosure is given by (1)

$$p(r, \theta) = i \frac{e^{i\pi/4}}{\sqrt{2\pi}} \dot{P}^+(-k \cos \theta, h) e^{ik \sin \theta h} \frac{e^{-ikr}}{\sqrt{kr}} \quad (4)$$

From Eqs. (1) and (4), the radiated sound pressure field is determined by the modal response coefficients of sound pressure and pressure gradient along the horizontal direction. To determine the coefficients, the continuity relations of sound pressure and pressure gradient at the opening of the unbaffled long enclosure are considered:

$$\begin{bmatrix} P_1 \\ P_2 \\ \vdots \\ P_n \end{bmatrix} = \begin{bmatrix} Y_1^C(y_1) & Y_2^C(y_1) & \cdots & Y_m^C(y_1) \\ \vdots & \vdots & \vdots & \vdots \\ Y_1^C(y_n) & Y_2^C(y_n) & \cdots & Y_m^C(y_n) \end{bmatrix} \begin{bmatrix} g_1 \\ g_2 \\ \vdots \\ g_m \end{bmatrix} \quad (5)$$

and

$$\begin{bmatrix} V_1 \\ V_2 \\ \vdots \\ V_n \end{bmatrix} = \begin{bmatrix} Y_1^C(y_1) & Y_2^C(y_1) & \cdots & Y_m^C(y_1) \\ \vdots & \vdots & \vdots & \vdots \\ Y_1^C(y_n) & Y_2^C(y_n) & \cdots & Y_m^C(y_n) \end{bmatrix} \begin{bmatrix} f_1 \\ f_2 \\ \vdots \\ f_m \end{bmatrix} \quad (6)$$

where P_n and V_n are the sound pressure and horizontal pressure gradient on meshing nodes $(0, y_n)$ along the enclosure opening. Modal function outside the long enclosure is denoted by Y_m^C which can be obtained by the Helmholtz equation and the boundary condition on the ground.

Rewriting Eq. (5) and Eq. (6) in matrix form, we have

$$P = MG \quad (7)$$

$$V = MF \quad (8)$$

where matrices P and V can be obtained using FEM while M can be constructed using Eq. (5). After solving Eqs. (7) and (8), the modal response coefficients G and F can be obtained. Then, the directivity pattern of the radiated sound pressure field can be calculated using Eqs. (1) and (4).

3. RESULTS AND ANALYSIS

3.1 Sound reduction performance of ZMPPA

An unbaffled long enclosure of 2 m in length and 0.2 m in height is considered here. A monopole point source is located at (-0.4, 0.1) m and the volume velocity strength is 0.01 m²/s. The far-field observation radius is 0.8 m and the observation angle is in the range of [0, 150] degrees. Besides, the speed of sound and density of the air are 340 m/s and 1.225 kg/m³, respectively. First, the sound pressure field inside the long enclosure is calculated using the FEM. To ensure the calculation accuracy of the model, the mesh grids along the opening are refined as presented in Figure 2. Besides,

a geometrical singularity exists at the enclosure edge, where the pressure gradient at this point may be wrong. Hence, more grids are needed near this point and the horizontal pressure gradient at this point is replaced by that of the nearest point in the following calculations. Such replacement may give rise to certain errors of the radiated sound pressure field. However, the direct use of the horizontal pressure gradient at the edge will lead to wrong results.

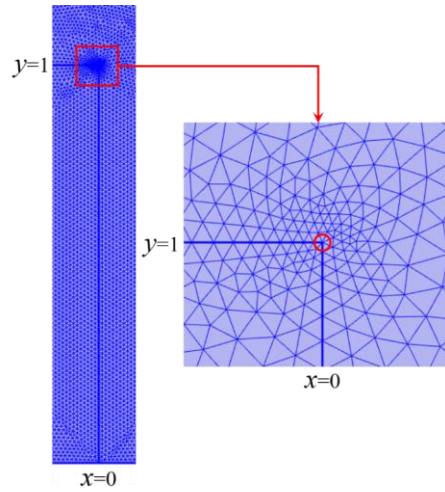


Figure 2 – Refinement of the meshing grids along the enclosure opening and at the sharp edge.

Comparison of SPLs at receivers outside long enclosures integrated with liners made of FMPPAs, CMPPAs, and ZMPPAs is presented in Figure 3. At the backside of the long enclosure as presented in Figure 3 (a) and Figure 3 (b), CMPPA and ZMPPA perform better than the FMPPA almost within the frequency range considered which indicates that the corrugated MPPAs can absorb more noise than the flat ones. Besides, ZMPPA performs better than the CMPPA when the frequency is above about 2000 Hz. This is attributed to the Z-shaped MPP profile which can absorb higher-order acoustical modes efficiently in the middle to high frequency range. In front of the long enclosure, as presented in Figure 3 (c), CMPPAs and ZMPPAs perform better than FMPPAs. However, ZMPPAs do not perform better than CMPPAs in the whole frequency range as the sound distribution in front of the enclosure is more complicated than that at the backside of the long enclosure.

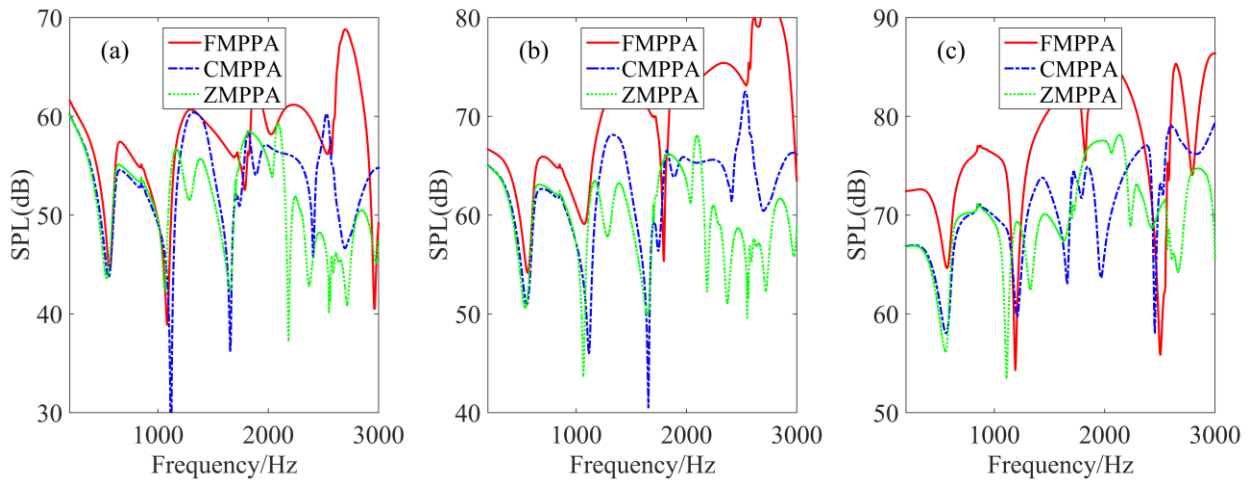


Figure 3 – Comparison of SPLs obtained by the liners made of FMPPAs, CMPPAs, and ZMPPAs at (a) $[-0.6, 0.6]$ m, (b) $[0, 0.6]$ m, and (c) $[0.6, 0.6]$ m.

The directivity patterns of the radiated SPL fields are shown in Figure 4. At 500 Hz, the SPLs of FMPPA, CMPPA, and ZMPPA are almost the same as the wavelength of the sound is much longer than the MPP shape size. Low frequency noise is difficult to be absorbed. ZMPPA performs slightly better than the CMPPA and FMPPA. At 2500 Hz, ZMPPA reduce the SPLs to a low level. The Z-

shaped MPP profile exhibit good performance in the absorption of higher-order acoustical modes. As a result, the radiated SPL outside the long enclosure is reduced significantly.

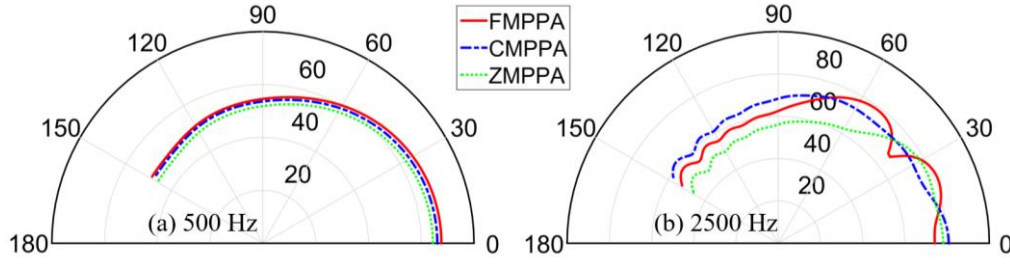


Figure 4 – Directivity patterns of the radiated SPL fields at (a) 500 Hz and (b) 2500 Hz.

3.2 Mechanism study

To explore the mechanism behind the sound absorption performance of the proposed ZMPPAs. The sound pressure along the opening and modal response coefficients at 500 Hz and 2500 Hz are presented in Figure 5 and Figure 6, respectively.

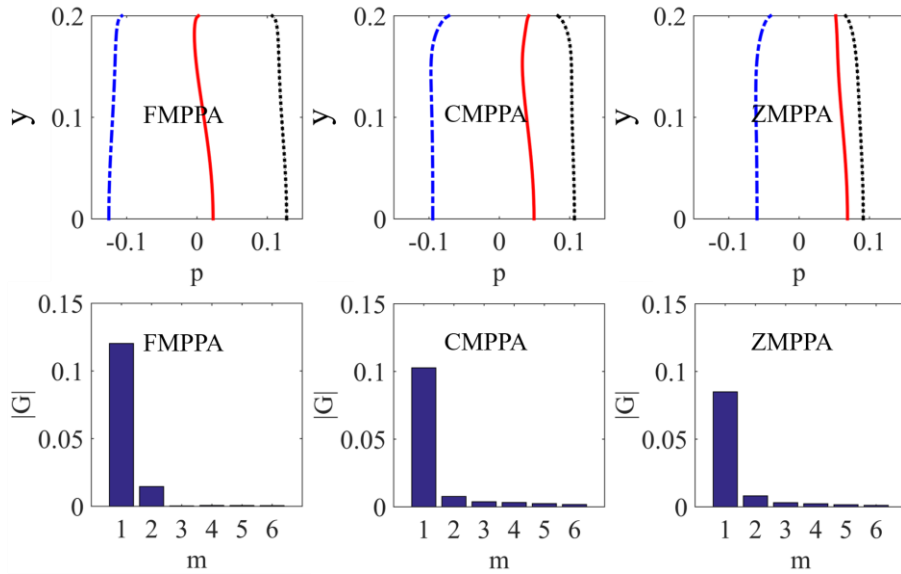


Figure 5 – Sound pressure along the opening and the modal response coefficients at 500 Hz.

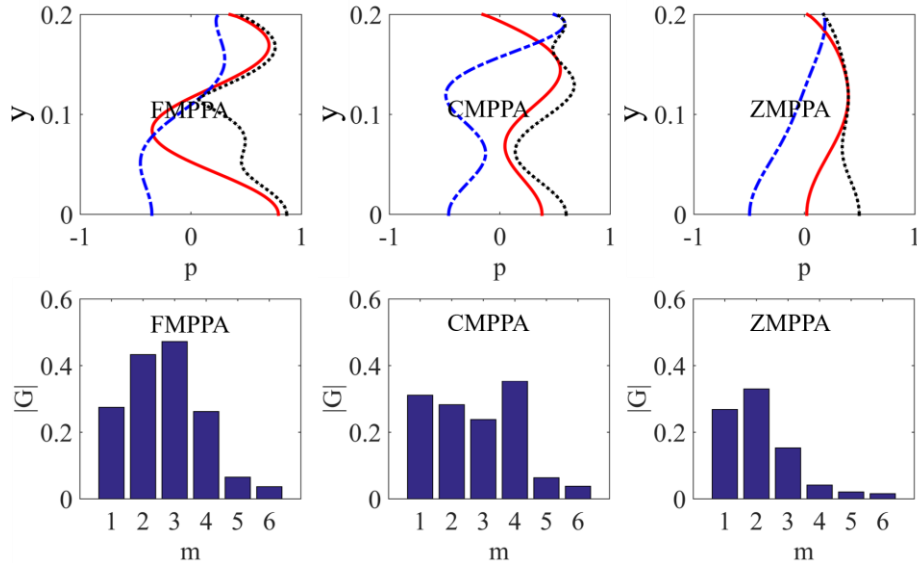


Figure 6 – Sound pressure along the opening and the modal response coefficients at 2500 Hz.

At 500 Hz, the absolute sound pressure along the opening is almost the same for MPPAs which are stand at around 0.1 Pa. Besides, the modal response coefficients demonstrates that the first mode is the dominant mode in these cases. However, the contribution of the mode in the ZMPPA case is smaller than those of FMPPA and CMPPA cases. As a result, the radiated sound field in ZMPPA case is also smaller than that of CMPPA and FMPPA cases. At 2500 Hz, multiple higher-order acoustical modes contribute to the sound field in FMPPA case. After integrating the CMPPA and ZMPPA, the modal response coefficients reduced a lot. In the ZMPPA case, only the first three modes contribute to the radiated sound pressure field and the amplitudes decrease significantly compared to that in FMPPA case. Therefore, the radiated sound field in the ZMPPA case is smaller than that in the CMPPA and FMPPA cases, which indicate that the proposed ZMPPA can absorb higher-order acoustical modes.

3.3 Experimental study

The performance of the ZMPPA, CMPPA, and FMPPA in reducing the radiated noise from an unbaffled long enclosure is examined using quasi-2D experiments. A schematic diagram of the test rig is presented in Ref. (1). The experiment is carried out in an anechoic chamber of 6 m in length, 6 m in width, and 3 m in height. As the proposed model was established in a 2D configuration, we designed a quasi-2D test rig accordingly (1, 12). It is constructed by two parallel arranged acrylic plates of 2.4 m long, 1.2 m wide, and 0.02 m thick. To eliminate the effect of the higher-order acoustical modes along vertical direction, the distance between the acrylic plates is kept at 0.04 m. Based on the cut-off rule of a channel, the plates can form a quasi-2D space under about 4250 Hz. A rectangular duct of 1.2 m long, 0.2 m wide, and 0.04 m high is inserted into the quasi-2D space to form an unbaffled long enclosure. To simulate the infinite region outside the long enclosure, a layer of wedge-shaped Melamine foam is placed at the side openings of the 2D space. The total heights of the wedges are 0.2 m. According to the rule of a quarter wavelength, they can achieve non-reflection boundaries above around 450 Hz. The whole test rig is supported by a frame assembled by aluminum extrusions. 2 A0 papers printed with the Cartesian and polar coordinate systems are pasted on the backside of the transparent acrylic plate to locate the measurement points. A Tannoy loudspeaker connected to a long pipe of 1 m in length and 25 mm in diameter is applied to simulate a monopole point source. Measurements of the directional characteristics of this source were conducted and it was observed that the deviations in all directions were within 1 dB for frequencies above about 200 Hz (13). The harmonic sound source is produced by a signal generator, output by an A/D converter (NI 4431), amplified by the power amplifier (LA 1201), and played by the Tannoy loudspeaker. Two microphones (B&K 4189) are connected to the conditioning amplifier (B&K NEXUS) and the data acquisition module (NI 9234). They move along the observation radius and collect acoustical signals every 5 degrees of observation angle. The testing system is controlled by LabVIEW which possesses the merits of good stability and high real-time performance in the targeted frequency range.

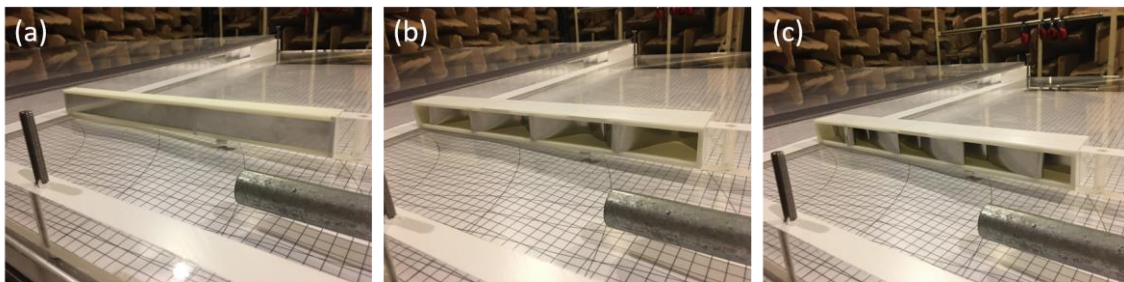


Figure 7 – Experimental setups. (a) a liner made of FMPPAs, (b) a liner made of CMPPAs, and (c) a liner made of ZMPPAs.

Here, 3 types of liners are mounting on the inner wall of the long enclosure as presented from Figure 7 (a) to Figure 7 (c). Each liner is assembled by four FMPPAs, CMPPAs, and ZMPPAs, respectively. The cavity width and depth of each unit are 100 mm and 60 mm, respectively. The corrugation depth and offset distance are 25 mm and 35 mm, respectively. A comparison between the ILs obtained by liners made of FMPPAs, CMPPAs, and ZMPPAs is demonstrated in Figure 8. From 500 Hz to 1600 Hz, the ILs are stands at about 5 dB to 8 dB which results from the shallow cavities of the MPPAs. Besides, in the frequency range of 1200 Hz to 1700 Hz, the FMPPAs outperform the CMPPAs and ZMPPAs. The liner made of ZMPPAs starts to show its advantages in the frequency range between 1700 Hz and 2000 Hz, in which high ILs are achieved. In this frequency interval, the

sound field inside the long enclosure become complex. Higher-order acoustical modes can be absorbed by the ZMPPAs.

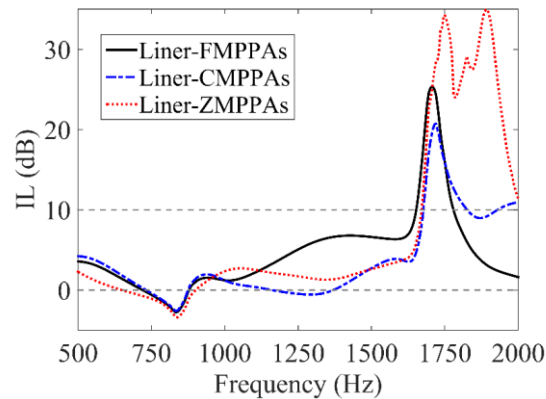


Figure 8 – Comparison of insertion losses obtained by liners made of FMPPAs, CMPPAs, and ZMPPAs.

4. CONCLUSIONS

In this paper, a hybrid method is established to calculate the sound radiated from an unbaffled long enclosure integrated with MPPAs. A liner consisting of multiple ZMPPAs is proposed to absorb higher order acoustical modes inside the long enclosure so that the radiated noise can be suppressed. The sound absorption performance of the ZMPPA is investigated which shows good performance in the middle to high frequency range. Further modal analysis demonstrates that the proposed ZMPPA can absorb higher order acoustical modes compared with that of FMPPA and CMPPA which shows great potential for the reduction of environmental noise. Finally, a quasi-2D experimental study is conducted which validates the proposed modal and verifies the numerical findings.

ACKNOWLEDGEMENTS

The authors would like to acknowledge the funding support from the Research Grants Council, Hong Kong (PolyU15209520).

REFERENCES

1. Yang, W. P, Choy, Y. S, Wang, Z. B, & Li, Y. (2022). Sound radiation and suppression of an unbaffled long enclosure using Helmholtz resonators. *Mechanical Systems and Signal Processing*, 165, 108408.
2. Law, M. K., Li, K. M., & Leung, C. W. (2008). Noise reduction in tunnels by hard rough surfaces. *The Journal of the Acoustical Society of America*, 124 (2), 961-972.
3. Eldredge, J. D. (2004). On the interaction of higher duct modes with a perforated liner system with bias flow. *Journal of Fluid Mechanics*, 510, 303-331.
4. Jing, X., Wang, X., & Sun, X. (2007). Broadband acoustic liner based on the mechanism of multiple cavity resonance. *AIAA journal*, 45(10), 2429-2437.
5. Zhou, D., Wang, X., Jing, X., & Sun, X. (2016). Acoustic properties of multiple cavity resonance liner for absorbing higher-order duct modes. *The Journal of the Acoustical Society of America*, 140(2), 1251-1267.
6. Wang, C., Cheng, L., Pan, J., & Yu, G. (2010). Sound absorption of a micro-perforated panel backed by an irregular-shaped cavity. *The Journal of the Acoustical Society of America*, 127(1), 238-246.
7. Gai, X. L., Xing, T., Li, X. H., Zhang, B., Wang, F., Cai, Z. N., & Han, Y. (2017). Sound absorption of microperforated panel with L shape division cavity structure. *Applied Acoustics*, 122, 41-50.
8. Yang, C., Cheng, L., & Pan, J. (2013). Absorption of oblique incidence sound by a finite micro-perforated panel absorber. *The Journal of the Acoustical Society of America*, 133(1), 201-209.
9. Wang, C., Huang, L., & Zhang, Y. (2014). Oblique incidence sound absorption of parallel arrangement of multiple micro-perforated panel absorbers in a periodic pattern. *Journal of*

Sound and Vibration, 333(25), 6828-6842.

10. Liu, Y., Zhang, Y., Chen, K., & Ma, X. (2020). Oblique incidence sound absorption of a hybrid structure using a micro-perforated panel and a planar actuator. *Applied Physics Express*, 13(5), 057001.
11. Wang, C., & Liu, X. (2020). Investigation of the acoustic properties of corrugated micro-perforated panel backed by a rigid wall. *Mechanical Systems and Signal Processing*, 140, 106699.
12. Guo, J., Zhang, X., Fang, Y., & Fattah, R. (2018). Reflected wave manipulation by inhomogeneous impedance via varying-depth acoustic liners. *Journal of Applied Physics*, 123(17), 174902.
13. Li, K. M., Kwok, M. P., & Law, M. K. (2008). A ray model for hard parallel noise barriers in high-rise cities. *The Journal of the Acoustical Society of America*, 123(1), 121-132.